2013 IEEE/RSJ International Conference on
Intelligent Robots and Systems (IROS)
November 3-7, 2013. Tokyo, Japan

"Anti-Fatigue" Control for Over-Actuated Bionic Arm with Muscle Force Constraints

Haiwei Dong[1], Setareh Yazdkhasti[2], Nadia Figueroa[1] and Abdulmotaleb El Saddik[1,3]

Abstract— **In this paper, we propose an "anti-fatigue" control method for bionic actuated systems. Specifically, the proposed method is illustrated on an over-actuated bionic arm. Our control method consists of two steps. In the first step, a set of linear equations is derived by connecting the acceleration description in both joint and muscle space. The pseudo inverse solution to these equations provides an initial optimal muscle force distribution. As a second step, we derive a gradient direction for muscle force redistribution. This allows the muscles to satisfy force constraints and generate an even distribution of forces throughout all the muscles (i.e. towards "anti-fatigue"). The overall proposed method is tested for a bending-stretching movement. We used two models (bionic arm with 6 and 10 muscles) to verify the method. The force distribution analysis verifies the "anti-fatigue" property of the computed muscle force. The efficiency comparison shows that the computational time does not increase significantly with the increase of muscle number. The tracking error statistics of the two models show the validity of the method.**

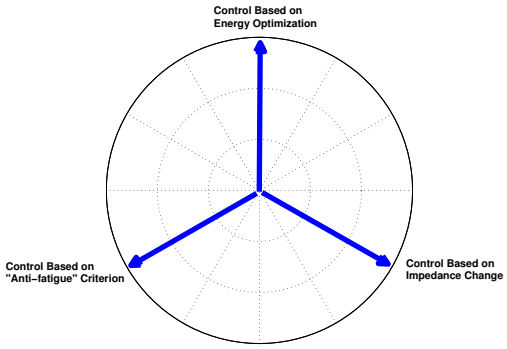

Fig. 1: Control method classification.

I. INTRODUCTION

The bionic arm is a human-like musculoskeletal structure that is activated by numerous muscles. It has many advantages, such as high robustness, low load for each muscle, etc. One important potential application for this bionic system, due to its similarity to the human arm, is the possibility to estimate/predict the human muscle force based on the control of the bionic system. Towards this objective, many bionic robots have been built so far, such as ECCEROBOT from University of Zurich [1], Kenshiro from University of Tokyo [2], Airic's Arm from Festo Co. Lt., Lucy from Vrije Universiteit Brussel [3].

However, controlling a bionic system is quite sophisticated compared to controlling a classical mechanical system. The main difficulty is that the bionic system is always actuated by numerous muscles [4], which makes it a redundant over-actuated nonlinear dynamic system [5]. The coordination of these muscles is not simple. Moreover, since muscles can provide only a "pull" force, the muscle force should remain positive and the output force for each muscle must be within an interval from 0 to maximum. This enforces muscle force constraints as another requisite in the control problem. Various approaches have been proposed to resolve this redundancy problem. In [6], inherent to redundant systems for internal force regarding the overall stability, a cable-driven system for a simple sensor-motor control scheme was proposed. As there exists redundancy in joint space, muscle space and impedance space, the solution of muscle coordination is not unique [5]. The possible solution for controlling the bionic arm can be concluded in three categories: optimizing energy consumption, impedance change and "anti-fatigue" (Fig.1).

For the first category (the optimization solution), the muscle coordination solutions differ depending on the chosen criteria. For example, in [7], the criterion of the minimum overall energy-consumption of muscles was considered. In [8], the trajectory of the arm is optimized and adjusted for a time and energy-optimal motion. In [9], dynamic optimization of minimum metabolic energy expenditure was used to solve the motion control of walking. In [10], a nonlinear optimal controller was used to develop a real-time EMG-driven virtual arm. However, optimization is often computationally demanding, and this can be a disadvantage for its usage in applications.

Regarding the second category (impedance change), as the muscles in the bionic arm are antagonist muscles, different arm stiffness can generate the same movement. The stiffness change can be achieved by impedance control. The impedance issue has been considered for years. Early work from the neurophysiology community presented a study where deafferented monkeys are shown to be capable of maintaining a posture under disturbances. Later on, many impedance control methods have been proposed. For example, in [11], the mechanical impedance property of muscles

[1]H. Dong and N. Figueroa are with Department of Engineering, New York University AD, P.O. Box 129188, Abu Dhabi, UAE {haiwei.dong; nadia.figueroa}@nyu.edu

[2]S. Yazdkhasti is with Al Ghurair University, Dubai Academic City, Dubai, UAE setareh@agu.ac.ae

[3]A. E. Saddik is with Department of Engineering, New York University AD and School of Electrical Engineering and Computer Science, University of Ottawa, 800 King Edward, Ottawa, Ontario, Canada elsaddik@uottawa.ca

was modeled based on adaptive impedance control, which was proposed in common physiological cases. In [12], the arm movement was achieved by shifting the equilibrium point gradually. Afterwards, this kind of impedance control scheme has been named equilibrium trajectory control, or virtual trajectory control [13]. In [14], a complete model of an arm with force and impedance characters was created for human-robot dynamic interaction.

The objective of the third category ("anti-fatigue") is to design the control in such a way that muscular fatigue is minimal. This is associated with finding a feasible solution targeted at distributing the muscle forces evenly. The "anti-fatigue" control is very important as it corresponds to the human's neuro control scheme. Until recently, this "anti-fatigue" control has not been fully considered. There are few research works on it. From these, the work in [15] is noteworthy, as they proposed a muscle force distribution method to drive the muscle forces to their mid-range in the sense of least-squares.

Another important factor to take into consideration while developing a muscle force control system for a bionic arm is the body movement patterns, as introduced in the neuro-science domain. The dynamics of the musculoskeletal system have an order parameter which can determine the phase transition of movements [16]. These scenarios were found in finger movement and limb movement patterns [17][18].

Actually, each category mentioned above points towards a separate solution space corresponding to a specific requirement. There exists overlapped solution spaces indicating the compromise of different requirements. The compromise method is a promising field in the future. In this paper, we focus on proposing an "anti-fatigue" solution to bionic arm control. Specifically, our control method consists of two steps. In the first step, the initial muscle force is derived by connecting the acceleration description in both joint and muscle space. As a second step we derive a gradient direction for muscle force redistribution. This allows the muscles to satisfy force constraints and generate an even distribution of forces throughout all the muscles (i.e. towards "anti-fatigue"). The overall proposed method is tested in two models (bionic arm with 6 and 10 muscles). The force distribution analysis, efficiency comparison and tracking error statistics verify the validity of the method.

The paper is organized as follows. In Section II, we begin by describing the mathematical model of a bionic arm. In Section III, our "anti-fatigue" muscle force control method is presented. A simulation with details of dynamic responses as well as efficiency and control performance evaluation is illustrated in Section IV. Finally, in Section V we will conclude this paper.

II. BIONIC ARM MODELING

A 2-dimensional bionic robot arm model was built based on the upper limb data of a digital human (Fig.2). The model is restricted in a horizontal plane and thus has two degrees of freedom (shoulder flexion-extension and elbow flexion-extension). The range of the shoulder angle is from

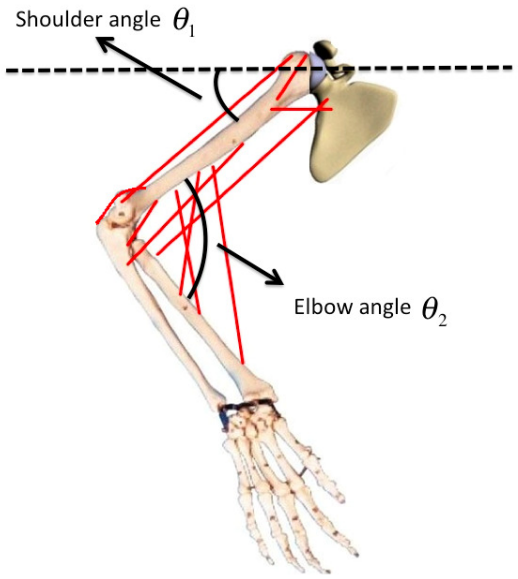

Fig. 2: Bionic arm model.

-20 to 100 degrees, and the range of the elbow is from 0 to 170 degrees. The bionic arm is driven by articular and monoarticular muscles. By considering the arm (including upper arm and lower arm) as a planar, two-link, articulated rigid object, the position of the hand can be derived by a 2-vector q of the shoulder and elbow angles. The input is a muscle force vector F_m. Due to the redundant muscles, the dynamics of the rigid object are strongly nonlinear. Using the Lagrangian equations from classical dynamics, we obtain the dynamic equations of the upper limb model as

$$\begin{bmatrix} H_{11}(t) & H_{12}(t) \\ H_{21}(t) & H_{22}(t) \end{bmatrix} \begin{bmatrix} \ddot{q}_1 \\ \ddot{q}_2 \end{bmatrix} + \begin{bmatrix} C_{11}(t) & C_{12}(t) \\ C_{21}(t) & C_{22}(t) \end{bmatrix} \begin{bmatrix} \dot{q}_1 \\ \dot{q}_2 \end{bmatrix} = \begin{bmatrix} \tau_1(t) \\ \tau_2(t) \end{bmatrix} \tag{1}$$

or abbreviated as

$$H(t)\ddot{q} + C(t)\dot{q} = \tau \tag{2}$$

with $q = \begin{bmatrix} q_1 & q_2 \end{bmatrix}^T = \begin{bmatrix} \theta_1 & \theta_2 \end{bmatrix}^T$ being the shoulder and elbow angles respectively. $\tau = \begin{bmatrix} \tau_1 & \tau_2 \end{bmatrix} = f(F_m)$ is the joint torque, which is considered as a function of muscle force F_m

$$F_m = \begin{bmatrix} F_{m,1} & F_{m,2} & \cdots & F_{m,n_{muscle}} \end{bmatrix}^T \tag{3}$$

where n_{muscle} is the muscle number. $H(q,t)$ is the inertia matrix which contains information with regards to the instantaneous mass distribution. $C(q,\dot{q},t)$ is the centripetal and coriolis torques representing the moments of centrifugal forces.

$$
\begin{aligned}
H_{11} &= J_1 + J_2 + m_2 d_1^2 + 2 m_2 d_1 c_2 \cos(q_2) \\
H_{12} &= H_{21} = J_2 + m_2 d_1 c_2 \cos(q_2) \\
H_{22} &= J_2 \\
C_{11} &= -2 m_2 d_1 c_2 \sin(q_2)\, \dot{q}_2 \\
C_{12} &= -m_2 d_1 c_2 \sin(q_2)\, \dot{q}_2 \\
C_{21} &= m_2 d_1 c_2 \sin(q_2)\, \dot{q}_1 \\
C_{22} &= 0
\end{aligned} \tag{4}
$$

where c_i is the distance from the center of a joint i to the center of gravity point of link i. d_i is the length of link i. $J_i = m_i d_i^2 + I_i$ where I_i is the moment of inertia about the axis through the center of the i-th link's mass m_i.

III. "ANTI-FATIGUE" CONTROL

A. Basic Idea

There are two steps to achieve "anti-fatigue" muscle force. In Step1, we use pseudo-inverse to compute the initial muscle force. The input is the desired joint trajectory and muscle force boundary. The output is the minimum muscle force under the sense of least-squares. The basic idea is to initially create a linear equation based on the description of the acceleration contribution in joint space and muscle space, respectively. Then, the muscle activation level is calculated by solving the above linear equation. Finally, the muscle force is computed by scaling the muscle activation level with the corresponding maximum muscle force.

Based on Eq.1, the general dynamic equation of the bionic arm can be written in the general form as

$$
H(q,t)\,\ddot{q} + C(q,t)\,\dot{q} = f(F_m) \tag{5}
$$

where $f(F_m)$ maps muscle force F_m to joint torque. The equation is simplified to the following form

$$
H(q,t)\,\ddot{q} = \Gamma + \Lambda \tag{6}
$$

Here, $\Gamma = f(F_m)$, $\Lambda = -C(q,t)\,\dot{q}$. From this viewpoint, we can separate the total acceleration contribution into two parts, i.e. $\ddot{q}_\Gamma$ and $\ddot{q}_\Lambda$. Thus, we have

$$
\ddot{q} = \ddot{q}_\Gamma + \ddot{q}_\Lambda \tag{7}
$$

where

$$
\ddot{q}_\Gamma = H(q,t)^{-1}\,\Gamma, \;\; \ddot{q}_\Lambda = H(q,t)^{-1}\,\Lambda
$$

The above equations indicate that in the joint space, the acceleration contribution comes from 1): joint torque Γ, 2): centripetal and coriolis torque Λ. Hence, we can compute the acceleration contribution from joint torque $\ddot{q}_\Gamma$ by Eq. 7. Whereas, from the muscle space viewpoint, each muscle has acceleration contribution. Assuming the total muscle number is n_{muscle}, the maximum acceleration contribution of the j-th $(1 \le j \le n_{muscle})$ muscle $\ddot{q}_{m,j,max}$ $(1 \le j \le n_{muscle})$ can be calculated as [15]

$$
\begin{aligned}
&\ddot{q}_{m,1,max} = H^{-1} J_m^T \; F_m|_{F_{m,1}=F_{m,1,max};F_{m,j}=0\,(j\neq 1)} \\
&\ddot{q}_{m,2,max} = H^{-1} J_m^T \; F_m|_{F_{m,2}=F_{m,2,max};F_{m,j}=0\,(j\neq 2)} \\
&\cdots \\
&\ddot{q}_{m,n_{muscle},max} = H^{-1} J_m^T \\
&\qquad F_m|_{F_{m,n_{muscle}}=F_{m,n_{muscle},max};F_{m,j}=0\,(j\neq n_{muscle})}
\end{aligned}
$$

By combining these two approaches for the computation of the acceleration contribution in joint space and muscle space, we can build a linear equation

$$
AX = B \tag{8}
$$

where

$$
\begin{aligned}
A &= \begin{bmatrix} \ddot{q}_{m,1,max} & \ddot{q}_{m,2,max} & \cdots & \ddot{q}_{m,n_{muscle},max} \end{bmatrix} \\
X &= \begin{bmatrix} \sigma_1 & \sigma_2 & \cdots & \sigma_{n_{muscle}} \end{bmatrix}^T \\
B &= \ddot{q}_\Gamma
\end{aligned}
$$

where X is a vector of muscle activation level σ_i $(i = 1, 2, ..., n_{muscle})$. The muscle activation level is a scalar in the interval $[0, 1]$, representing the percentage of maximum contraction force of each muscle. Therefore, the muscle force can be calculated as a product of maximum contraction force and activation level. Considering Eq.8, we can use the pseudo-inverse to compute muscle activation level

$$
X = A^+ B \tag{9}
$$

where $A^+ = A^T \left(A A^T\right)^{-1}$. To calculate the muscle force F_m, we define

$$
F_{m,max} = \begin{bmatrix} F_{m,1,max} & \cdots & F_{m,n_{muscle},max} \end{bmatrix}^T \tag{10}
$$

as the maximum muscle force vector. The muscle force can be calculated as the product of the muscle activation level and maximum muscle force. Thus, the initial optimized muscle force can be computed as

$$
F_{m,ini} = F_{m,max} \otimes X \tag{11}
$$

where the operator $\otimes$ calculates the dot product of two vectors. Similarly, due of the pseudo-inverse property, the initial muscle force satisfies the minimum of the muscle force in the least-squares sense, i.e.,

$$
min \left\| F_{m,ini} \right\|_2 = min \left(\sum_{j=1}^{n_{muscle}} F_{m,ini,j}^2 \right) \tag{12}
$$

The computed initial muscle force $F_{m,ini}$ does not consider the physical constraints of the muscles, which are: 1) the maximum output muscle force is limited and 2) muscles can only contract (i.e. non-negative force values). The objective in Step2 is to make the muscles work in an "anti-fatigue" manner (i.e., the load is distributed evenly). Here, we use gradient descent to generate resulting muscle

forces that satisfy the above constraints. This is achieved by providing a gradient direction in the null space of the pseudo-inverse solution obtained in Step1 to relocate the initial muscle force $F_{m,ini}$ to an optimized state, which satisfies muscle constraints 1) and 2).

We assume each muscle force is limited to an interval from $F_{m,j,min}$ to $F_{m,j,max}$ for $(1 \leq j \leq n_{muscle})$. Our objective is to find a gradient direction that bounds each muscle force $F_{m,j}$ to a value equal or greater than $F_{m,j,min}$, and equal or less than $F_{m,j,max}$. To consider both the muscle fatigue issue and the muscle force boundary constraint, the output force of each muscle can be limited to be around the middle between $F_{m,j,min}$ and $F_{m,j,max}$, i.e. the mid-range of the muscle force constraints. The physical meaning of this method is to distribute the overall load to all the muscles averagely, allowing each muscle to work around its appropriate working load. Based on this "anti-fatigue" load distribution principle, the muscles can continually work for extended time periods. According to the above muscle force distribution principle, to generate the gradient direction, we choose a function h which represents the sum of squared deviation of the current muscle force and its middle force

$$h\left(F_m\right) = \sum_{j=1}^{n_{muscle}} \left(\frac{F_{m,j} - F_{m,j,mid}}{F_{m,j,mid} - F_{m,j,max}} \right)^2 \tag{13}$$

where

$$\begin{aligned} & 0 \leq F_{m,j,min} \leq F_{m,j} \leq F_{m,j,max} \\ & F_{m,j,mid} = \frac{F_{m,j,min} + F_{m,j,max}}{2} \\ & j = 1, 2, \cdots, n_{muscle} \end{aligned}$$

We define F_{in} as a vector representing the internal force of muscles generated by redundant muscles which has the same dimension with F_m. We calculate F_{in} as the gradient of the function h, i.e.,

$$\begin{aligned} F_{in} &= K_{in} \left. \frac{\partial h\left(F_m\right)}{\partial F_m} \right|_{F_{m,ini}} = K_{in} \left. \nabla_h \right|_{F_{m,ini}} \\ &= K_{in} \begin{bmatrix} 2\frac{F_{m,ini,1} - F_{m,1,mid}}{F_{m,1,mid} - F_{m,1,max}} \\ 2\frac{F_{m,ini,2} - F_{m,2,mid}}{F_{m,2,mid} - F_{m,2,max}} \\ \vdots \\ 2\frac{F_{m,ini,n_{muscle}} - F_{m,n_{muscle},mid}}{F_{m,n_{muscle},mid} - F_{m,n_{muscle},max}} \end{bmatrix} \end{aligned} \tag{14}$$

where K_{in} is a scalar matrix controlling the optimization speed. It is easy to prove that the direction of F_{in} points to $F_{m,i,mid}$. Therefore, we map the internal force F_{in} into F_m space, i.e., pseudo-inverse solution's null space as

$$g\left(F_{in}\right) = \left(I - \left(J_m^T\right)^+ J_m^T \right) F_{in} \tag{15}$$

where I is an identity matrix having the same dimension as the muscle space. According to the Moore-Penrose pseudo-inverse, $g\left(F_{in}\right)$ is orthogonal with the space of $F_{m,ini}$. Finally, the optimized muscle force is calculated as

$$F_m = F_{m,ini} + g\left(F_{in}\right) \tag{16}$$

It is noted that, the main computational burden in the muscle force optimization is the pseudo-inverse calculation (Eq.9), especially in the inverse computation $\left(AA^T\right)^{-1}$. An advantage of this formulation is that the dimension of $\left(AA^T\right)^{-1}$ is equal to the joint dimension. Thus, with the increase of muscle number, the computational burden does not increase significantly. This is verified in the simulation section (Section IV).

B. Procedures

The block diagram of the proposed method is shown in Fig.3. The input is the desired trajectory of joint and muscle force constraints. The output is the muscle force. There are two main computational steps. In Step1, we use pseudo-inverse to calculate the initial muscle force. In Step2, the internal force is calculated and further mapped into the null space of the pseudo-inverse solution in Step1. The final output of the muscle force is the sum of the calculation results in Step1 and Step2. The detailed procedures of the proposed method are shown in Algorithm 1.

Algorithm 1: "Anti-fatigue" Muscle Force Control

INPUT: The desired trajectory points and muscle force boundary.

OUTPUT: The Optimized muscle force.

- Procedure1: Generating desired trajectory

Given the desired trajectory points, by using QR decomposition, we can formulate a continuous derivative function to connect trajectory points at each moment in time [5]

$$q_d\left(t_k\right) = a_k t_k^3 + b_k t_k^2 + c_k t_k + d_k \tag{17}$$

Then the desired trajectory position, velocity and acceleration $\begin{bmatrix} q_d\left(t_k\right) & \dot{q}_d\left(t_k\right) & \ddot{q}_d\left(t_k\right) \end{bmatrix}^T$ are computed at time t_k by the derivative calculation

$$\dot{q}_d\left(t_k\right) = 3a_k t_k^2 + 2b_k t_k + c_k \tag{18}$$

$$\ddot{q}\left(t_k\right) = 6a_k t_k + 2b_k \tag{19}$$

- Procedure2: Preparing A and B

To calculate the initial optimized muscle force, we need to prepare the acceleration contribution matrix from the muscle space A and the acceleration contribution from joint space B.

$$A = \begin{bmatrix} \ddot{q}_{m,1,max} & \ddot{q}_{m,2,max} & \cdots & \ddot{q}_{m,n_{muscle},max} \end{bmatrix} \tag{20}$$

where $\ddot{q}_{m,j,max}$ $(j = 1, 2, \cdots, n_{muscle})$ can be specified as

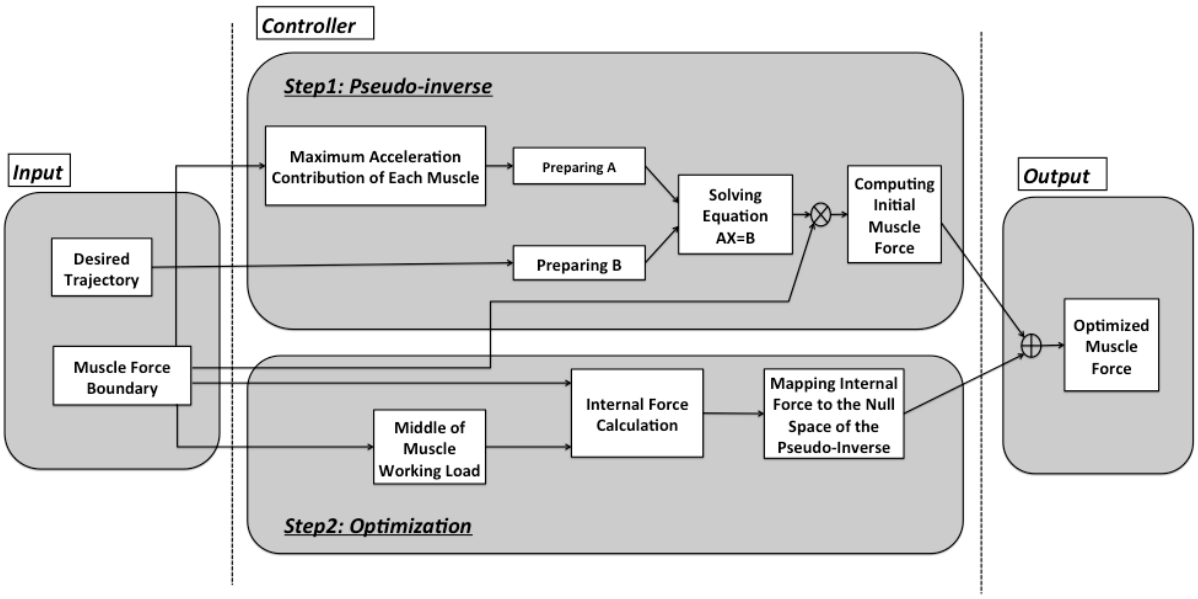

Fig. 3: Block diagram of the algorithm.

$$\ddot{q}_{m,1,max} = H(q,t)^{-1} J_m^T \cdot \begin{bmatrix} F_{m,1,max} & 0 & \cdots & 0 \end{bmatrix}^T$$
$$\ddot{q}_{m,2,max} = H(q,t)^{-1} J_m^T \cdot \begin{bmatrix} 0 & F_{m,2,max} & \cdots & 0 \end{bmatrix}^T$$
$$\cdots$$
$$\ddot{q}_{m,n_{muscle},max} = H(q,t)^{-1} J_m^T \cdot \begin{bmatrix} 0 & 0 & \cdots & F_{m,n_{muscle},max} \end{bmatrix}^T$$

where J_m is the Jacobian matrix from muscle space to joint space. According to Eq.7, B can be computed as

$$B = \ddot{q}_\Gamma = \ddot{q}|_{q_d,\dot{q}_d,\ddot{q}_d} - \ddot{q}_\Lambda = \ddot{q}|_{q_d,\dot{q}_d,\ddot{q}_d} - H(q,t)^{-1}\Lambda \quad (21)$$

- Procedure3: Muscle force optimization

First, we compute the initial optimized muscle force by pseudo-inverse. Based on the previously computed A and B in Procedure2, we can obtain the initial muscle activation level as follows

$$X = \begin{bmatrix} \sigma_1 & \sigma_2 & \cdots & \sigma_{n_{muscle}} \end{bmatrix}^T = A^+ B \quad (22)$$

where $A^+ = A^T \left(AA^T\right)^{-1}$. Then, the initial optimized muscle force is

$$F_{m,ini} = F_{m,max} \otimes X \quad (23)$$
$$= \begin{bmatrix} F_{m,1,max}\sigma_1 & \cdots & F_{m,n_{muscle},max}\sigma_{n_{muscle}} \end{bmatrix}^T$$

Second, we re-optimize the muscle force (e.g. distributing muscle force evenly) by gradient descent. The final muscle force is

$$F_m = F_{m,ini} + \left(I - \left(J_m^T\right)^+ J_m^T\right) \cdot K_{in} \begin{bmatrix} 2\frac{F_{m,ini,1}-F_{m,1,mid}}{F_{m,1,mid}-F_{m,1,max}} \\ 2\frac{F_{m,ini,2}-F_{m,2,mid}}{F_{m,2,mid}-F_{m,2,max}} \\ \vdots \\ 2\frac{F_{m,ini,n_{muscle}}-F_{m,n_{muscle},mid}}{F_{m,n_{muscle},mid}-F_{m,n_{muscle},max}} \end{bmatrix} \quad (24)$$

where K_{in} is a scalar matrix controlling the optimization speed. I is an identity matrix having the dimension of n_{muscle}.

IV. SIMULATION

The performance of the proposed muscle force computation method was tested through a bending-stretching simulation. According to the bending-stretching movement, the desired trajectory points of the shoulder joint and elbow joint are generated with a sine wave signal. These trajectory points are used to create a trajectory function for each joint. By applying the computed muscle force, the bionic arm is controlled. The desired movement is bending the upper arm from 0 rad to $\pi/2$ rad and the lower arm from 0 rad to $\pi/3$ rad, and then stretching them back to 0 rad. The frequency of the movement is 2π Hz and the total simulation time is 10s. The muscle force constraint is set from 0 to 500N. In this simulation, we use bionic arms with 6 and 10 muscles to test the proposed method on force distribution, tracking capability, and efficiency.

A. Settings of the Bionic Arm with 6 Muscles

The inertia-related parameters of the 6-muscle bionic arm are based on real data of a human upper limb. The muscle configuration, coordinate setting and inertia-related coefficients settings are shown in Fig.4(a) and Table I.

Segment	Upper Arm	Lower Arm
Length (m)	0.282	0.269
Mass (kg)	1.980	1.180
MCS Pos (m)	0.163	0.123
I_{11} $(kg \cdot m^2)$	0.013	0.007
I_{22} $(kg \cdot m^2)$	0.004	0.001
I_{33} $(kg \cdot m^2)$	0.011	0.006

TABLE I: Anthropological parameter values. (MCS Pos means mass center position.)

Muscle Index	Muscle Name	Coordinate Parameter	Attached Bones
1	Brachioradialis	a101=0.182, a102=0.065	O:Humeral, I:Radius
2	Brachialis	a71=0.13, a72=0.021	O:Humeral, I:Ulna
3	Triceps	a51=0.015, a52=0.02	O:Scapula, I:Ulna
4	Coracobrach	a11=0.01, a12=0.056	O:Scapula, I:Humeral
5	Deltoid	a21=0.01, a22=0.07	O:Scapula, I:Humeral
6	Pronators	a91=0.117, a92=0.024	O:Humeral, I:Radius
7	Bicep	a31=0.045, a32=0.02	O:Scapula, I:Radius
8	Supinator	a81=0.08, a82=0.028	O:Humeral, I:Radius
9	Ancones	a61=0.01, a62=0.01	O:Humeral, I:Ulna
10	Media brachial	a41=0.01, a42=0.01	O:Humeral, I:Ulna

TABLE II: Muscle configuration of the bionic arm with 10 muscles. (O: the attached bone with the original site; I: the attached bone with the insertion site.)

We extracted the anthropological data from [19]. In this model, we consider the common-used bionic arm with mono-articular and bi-articular muscles. In this model there are 6 muscles: four of them are mono-articular and two are bi-articular. Without loss of generality, the muscle configuration coefficients are set as $a_{ij} = 0.1m$ $(1 \leq i \leq 6, 1 \leq j \leq 2)$ [15].

B. Settings of the Bionic Arm with 10 Muscles

The muscle configuration of the 10-muscle bionic arm is based on real human musculoskeletal data. The muscle configuration is shown in Fig.4(b). Here, we use the same inertia coefficients with 6-muscle model (Table I). The muscles' origin, insertion coordinates and attached bones are shown in Table II. The attachment position of the muscles are determined from the digitized muscle insertions and anatomical descriptions. In this paper, we modified the model data in [20] to a 2D case and the new coordinates of each muscle's origin and insertion have been slightly extracted.

C. Force Distribution Comparison

The muscle force distribution is shown in Fig.5 where for each subfigure, m_i $(i = 1, 2, \cdots)$ indicates the i-th muscle. The vertical axis gives the statistical average muscle force in N. The upper and lower two subfigures show the computed

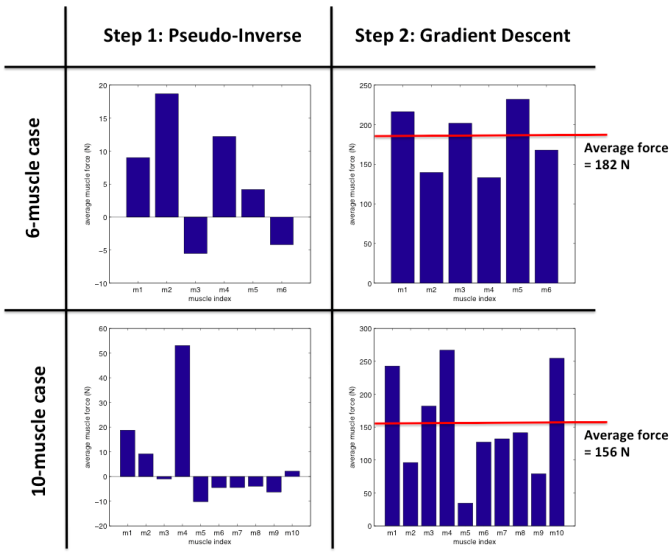

Fig. 5: Muscle force distribution.

muscle force based on the bionic arm with 6 muscles and 10 muscles, respectively. The left and right subfigures show the muscle force distribution in the Step1 and Step2. From this figure, we can conclude the following: 1) The muscle force distribution in Step2 is more evenly distributed than that in Step1; 2) In Step2, all the muscle forces satisfy the constraints, i.e. non-negative and within the output force boundary; 3) The computed average muscle force in the 10-muscle's case is smaller than that in 6-muscle's case, which verifies the fact that more muscles can lead to smaller load share.

D. Tracking Error and Visualization

The tracking error statistics for the 6-muscle's case and 10 muscle's case are shown in Fig.6. The horizontal axis lists the shoulder/elbow angles based on 6-muscle's case and shoulder/elbow angles based on 10-muscle's case. The vertical axis is the tracking error statistics in radians. In each box, the central mark indicates the median, the edges of the box show the 25 and 75 percentiles, respectively. It is shown that the tracking error of the shoulder and elbow angle in the 6 muscle's case and the 10 muscle's case is small (less than 0.01 rad). As the shoulder joint is the base joint of the elbow joint, the tracking error of the elbow joint is smaller for both cases. We can also see that, the tracking performance remains acceptable with the increase of the muscle number. For movement visualization, we used the Muscular Skeletal Modeling Software (MSMS) to create visible geometrical model of the arm's muscles and further evaluate the movement. In Fig.7, we provide snapshots of the arm movement from different viewpoints at one moment.

E. Computational Time Comparison

The computational time based on the bionic arm model with 6 muscles and 10 is compared. The simulation was run in a MacBook Air laptop. The basic configuration of the computer is listed below: processor: 1.7GHz Intel

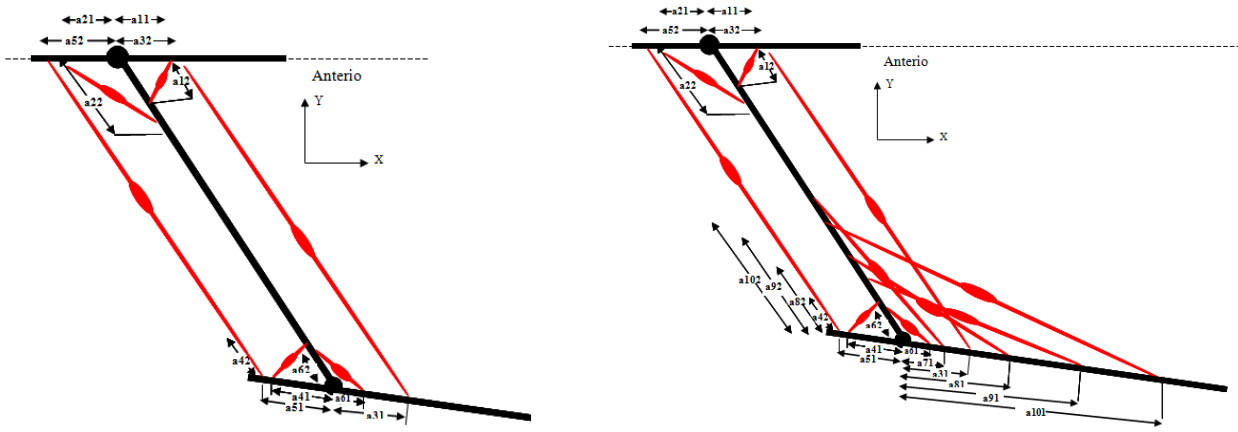

(a) With 6 muscles.

(b) With 10 muscles.

Fig. 4: Muscle configuration of the bionic arm.

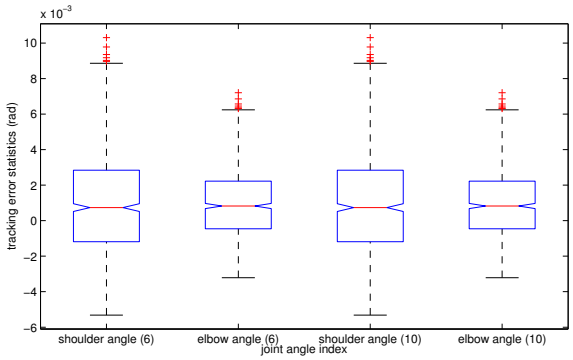

Fig. 6: Tracking error statistics.

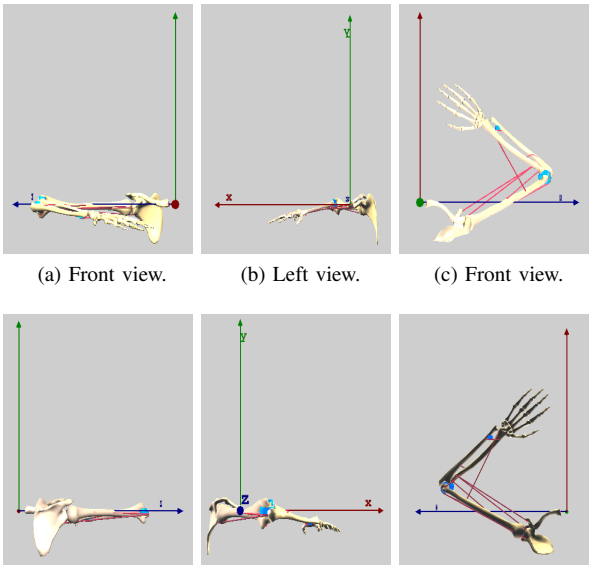

(a) Front view. (b) Left view. (c) Front view.

(d) Back view. (e) Right view. (f) Bottom view.

Fig. 7: Snapshots of the arm movement from different viewpoints.

Core i5; memory: 4GB 1333 MHz DDR3; startup disk: Macintosh HD 200GB; operation system: Mac OS X Lion 10.7.4 (11E53). Fig.8 shows that the computational time increases rather slightly (about 15%) considering that the muscle number increases heavily (67%). This indicates an advantageous property of our proposed method: the main computation regarding matrix calculation is in joint space and thus, the muscle number does not affect the efficiency significantly. On the other hand, the computational time is approximately half of the time in the simulated dynamic system, which means that the proposed method can be run in real-time.

V. DISCUSSION

In this paper, we use optimization to solve the redundancy problem in muscle coordination by avoiding complex computation and large computational burden. Generally, there have been two basic research methods to analyze muscle coordination: theory-oriented and experiment-oriented. Theory-oriented methods usually rely on modeling and optimization which can provide a rigorous optimized solution for coordination in a certain criterion. However, as the nonlinear optimization is usually a NP-hard problem, the optimized solution search has a high computational cost. On the other hand, experiment-oriented methods start from analyzing the electromyography pattern and mimic the real muscle activation signals. These kind of methods are usually designed for a specific system with certain mechanical structures. Our method belongs to the theory-oriented category, whereas we try to approach a "natural optimization", meaning that the optimization does not require many settings and complex time-consuming computation. as the main computation happens through the matrix inversion

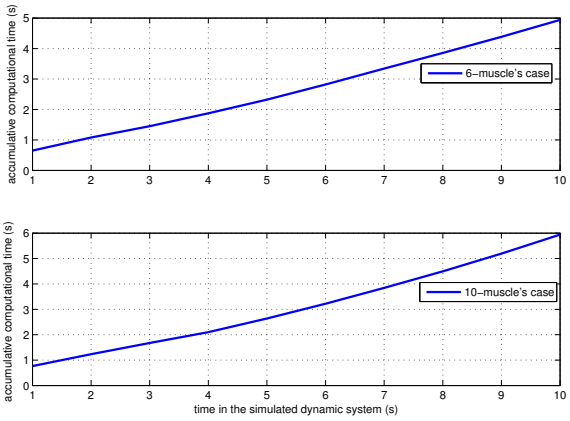

Fig. 8: Comparison of cumulative computational time between bionic arm with 6 muscles and that with 10 muscles.

of AA^T and $J_m^T J_m$, the computational scale of the proposed method is mainly related to the number of the joints, not to the number of muscles. This means that for more complex 3D musculoskeletal systems, even if we add more muscles, the computational time would not increase significantly.

VI. CONCLUSION

This paper presented a new method for "anti-fatigue" control of a bionic arm. The method consists of two main steps: first, a pseudo-inverse solution is utilized towards computing the initial muscle forces; and second, gradient descent is used to comply with the "anti-fatigue" requirement and distribute the muscle force while satisfying the constraints. The two arm movement simulations that we performed, the first with 6 muscles and the second with 10 muscles not only show the "anti-fatigue" property of the proposed method, but also indicate that the method has a desirable efficiency regarding scaling of the number of muscles. Quite importantly, the proposed method can also be readily generalized to numerous other bionic systems. Finally, our current directions for extensions and future work are centered on applying our method to a real-world robot, as well as investigating the relation of the computed muscle forces from our method to real muscle activation signals derived through Electromyography (EMG). Thus, turning our method also into a tool not only for synthesis of activation signals, but also for analysis of human motion observations.

REFERENCES

[1] V. Potkonjak, M. Jovanovic, P. Milosavljevic, N. Bascarevic, and O. Holland, "The puller-follower control concept in the multi-jointed robot body with antagonistically coupled compliant drives," in *Proceeding of IASTED International Conference on Robotics*, pp. 375–381, 2011.

[2] Y. Nakanish, Y. Asano, T. Kozuki, H. Mizoguchi, Y. Motegi, M. Osada, T. Shirai, J. Urata, K. Okada, and M. Inaba, "Design concep of detail musculoskeletal humanoid "kenshiro" - toward a real human body musculoskeletal simulator -," in *Proceeding of 12th IEEE-RAS International Conference on Humanoid Robots*, pp. 1–6, 2012.

[3] V. Bram, V. Ronald, V. Bjorn, V. Michael, and L. DIRK, "Overview of the lucy project: dynamic stabilization of a biped powered by pneumatic artificial muscles," *Advanced Robotics*, vol. 22, pp. 1027–1051, 2012.

[4] J. Lee, B. Yi, and J. Lee, "Adjustable spring mechanisms inspired by human musculoskeletal structure," *Mechanism and Machine Theory*, vol. 54, no. 76-98, 2012.

[5] G. Yamaguchi, *Dynamic Modeling of Musculoskeletal Motion: A Vectorized Appoach for Biomechanical Analysis in Three Dimensions*. Springer, 2005.

[6] K. Tahara, Z. Luo, S. Arimoto, and H. Kino, "Sensory-motor control mechanism for reaching movements of a redundant musculo-skeletal arm," *Journal of Robotic Systems*, vol. 22, pp. 639–651, 2005.

[7] M. Pandy, "Computer modeling and simulation of human movement," *Annual Review of Biomedical Engineering*, vol. 3, pp. 245–273, 2001.

[8] A. Heim and O. Stryk, "Trajectory optimization of industrial robots with application to computer aided robotics and robot controllers," *Optimization*, vol. 47, pp. 407–420, 2000.

[9] F. Anderson and M. Pandy, "Dynamic optimization of human walking," *Journal of Biomechanical Engineering*, vol. 125, pp. 381–390, 2001.

[10] K. Manal, R. Gonzalez, D. Lloyd, and T. Buchanan, "A real-time emg-driven virtual arm," *Computers in Biology and Medicine*, vol. 32, pp. 25–36, 2002.

[11] N. Hogan, "Adaptive control of mechanical impedance by coactivation of antagonist muscles," *IEEE Transactions on Automatic Control*, vol. 29, pp. 681–690, 1984.

[12] T. Flash, "The control of hand equilibrium trajectories," *Biological Cybernetics*, vol. 57, pp. 257–274, 1987.

[13] M. Katayama and K. M, "Virtual trajectory and stiffness ellipse during multijoint arm movement predicted by neural inverse models," *Biological Cybernetics*, vol. 69, pp. 353–362, 1993.

[14] K. Tee, E. Burdet, C. Chew, and T. Milner, "A model of force and impedance in human arm movements," *Biological Cybernetics*, vol. 90, pp. 368–375, 2004.

[15] H. Dong and N. Mavridis, "Adaptive biarticular muscle force control for humanoid robot arms," in *Proceeding of 12th IEEE-RAS International Conference on Humanoid Robots*, pp. 284–290, 2012.

[16] J. Kelso, *Dynamic Patterns*. MIT Press, 1995.

[17] J. Kelso, J. Buchanan, and S. Wallace, "Order parameters for the neural organization of single, multijoint limb movement patterns," *Experimental Brain Research*, vol. 85, pp. 432–444, 1991.

[18] H. Hanken, J. Kelso, and H. Bunz, "A theoretical model of phase thansitions in human hand movements," *Biological Cybernetics*, vol. 51, pp. 347–356, 1985.

[19] A. Nagano, S. Yoshioka, T. Komura, R. Himeno, and S. Fukashiro, "A three-dimensional linked segment model of the whole human body," *International Journal of Sport and Health Science*, vol. 3, pp. 311–325, 2005.

[20] W. Maurel, D. Thalmann, P. Hoffmeyer, P. Beylot, P. Gingins, P. Kalra, N. Magnenat, and P. Hoffmeyer, "A biomechanical musculoskeletal model of human upper limb for dynamic simulation," in *Proceedings of the Eurographics Computer Animation and Simulation Workshop*, 1996.